Vol. 07, No. 1 (2025) 267-272, doi: 10.24874/PES07.01B.005

Proceedings on Engineering Sciences

www.pesjournal.net

SYNTHESIS AND PHOTOLUMINESCENCE STUDIES OF YTTRIUM ZIRCONATE (YZO) PHOSPHORS POWDERS DOPED WITH BI^{3+} IONS

K. Suresh[1]
A. Ganesh
B. V. Naveen Kumar
C. V. Krishna Reddy

Received 12.11.2023.
Revised 26.12.2023.
Accepted 05.02.2024.

Keywords:

Photoluminescence, Emission, Excitation, Concentration Quenching, Chromaticity

A B S T R A C T

In this research work, Yttrium Zirconate ($Y_2Zr_2O_7$=YZO) phosphors doped with varying percentages of Bi^{3+} ions (x = 1.0, 1.5, 2.0, and 2.5) were successfully synthesized using a simple co-precipitation method and subsequently annealed at 1300°C. Through X-ray diffraction, it was determined that the pure YZO sample had an average crystallite size of 20.63 nm, whereas the Bi^{3+} doped YZO samples averaged at 18.36 nm. Scanning electron microscopy (SEM) revealed the prepared samples as spherical agglomerates with particle sizes ranging between 110 nm and 120 nm. Exciting the samples at a UV wavelength of 305 nm, the photoluminescence emission spectra displayed a peak at 430 nm (blue), attributed to the $^3P_1 \rightarrow {}^1S_0$ transition of Bi^{3+} ions. Emission intensity decreased beyond a doping concentration of 1.5 at. % Bi^{3+}, indicating a concentration quenching effect, establishing the optimal doping concentration at 1.5 at.%. Additionally, CIE color chromatic parameters were computed for the Bi^{3+} doped samples, pinpointing the optimized Bi^{3+} content (1.5 at. %) within the "Cyan" region, showcasing its potential for use in near-ultraviolet (NUV) blue emitting chips for display applications.

1. INTRODUCTION

Yttrium zirconate ($Y_2Zr_2O_7$ = YZO) is a promising fluorescent material with a wide bandgap (5.3 eV) and excellent chemical stability (Zhang, Lü, Qiu, Zhou, & Ma, 2008). It has been extensively studied as a host for several rare earth dopants such as Eu^{3+}, Dy^{3+} and Tb^{3+} that emit visible light when excited with UV radiation (Q. Du, Zhou, Zhou, Jia, & Zhou, 2013; Gao et al., 2011; Papan, Vuković, Ahrenkiel, Jovanović, & Dramićanin, 2017). This type of mixed oxide is usually from the pyrochlore system (space group Fd-3m) or the fluorite system (space group Fm-3m). As the bond radius ratio decreases, the structure of $A_2B_2O_7$ gradually changes from fully ordered pyrochlore structure to disordered defective pyrochlore structures (Q. Du, Zhou, Zhou, & Yang, 2012; Xiao et al., 2021). The material exhibits remarkable optical transparency across an extensive wavelength range. Its substantial unit cell allows for extensive doping with trivalent lanthanide elements. Moreover, it can be co-doped with Bi^{3+} or Ce^{3+} to enhance fluorescence sensitivity (Ting, Chiu, Chang, & Chuang, 2011; Tong, Chen, Wang, & Huo, 2015).

Bi^{3+} ions are also known as photoactive activators and have been used to activate various host networks including YZO. When doped in YZO, Bi^{3+} ions can emit blue light through the $^3P_1 \rightarrow {}^1S_0$ (Whittle, Cranswick,

[1] Corresponding author: Kurudi Suresh
Email: kurudisuresh@gmail.com

Redfern, Swainson, & Lumpkin, 2009) transition. According to the results of many researchers, the emission spectra of Bi^{3+} ions are broad and the peaks range from blue to green for different host lattices, because the outer $6S^2$ electronic structures of Bi^{3+} ions depend on their environmental conditions, namely covalent and coordination No. etc. and place are equal. Therefore, from the results, Bi^{3+} ions can be used as a sensitizer to transfer their energy to the surrounding dopant ions and increase the doping emission intensity. Therefore, Bi^{3+} ion proved to be a very good sensitizer for common rare earth ions such as Eu^{3+}, Tb^{3+} and Dy^{3+} etc., with greatly enhanced fluorescence efficiency through energy transfer and broadening of excitation spectrum (Awater & Dorenbos, 2017; Q. Du et al., 2012; Talari, Chirauri, Rambabu, & Ramachandra Rao, 2023; Talari, Chirauri, Reddy, & Rao, 2022). In this study, the synthesis and photoluminescence properties of YZO phosphors with different doping concentrations of Bi^{3+} ions (X = 1.0, 1.5, 2.0 and 2.5) are reported.

These phosphors were synthesized through a straightforward co-precipitation process, which is of low cost, very effective in comparison with other chemical synthesis methods such as “polyol” or “sol-gel”. The precipitate formation in this method is often quick and the chemicals get well mixed in the solution forming a homogenous final product which is then subsequently annealed at 1300°C.

The crystal structure, morphology, and photoluminescence characteristics were examined using X-ray diffraction (XRD), scanning electron microscopy (SEM), and photoluminescence spectroscopy.

2. SYNTHESIS PROCEDURE

A straightforward wet-chemical technique called the "Co-Precipitation method" was used to prepare the samples of undoped and Bi^{3+} doped YZO phosphors. The $Y(NO_3)_3.6H_2O$, $Zr(NO_3)_3.6H_2O$, and $Bi(NO_3)_3.5H_2O$ precursors used in the production of YZO were bought from Sigma-Aldrich in 99.99% purity. The above-mentioned powders were weighed in the appropriate amounts and properly combined with 20 milliliters of distilled water in a round-bottom flask to create YZO in pure form. This concoction was placed on a heated magnetic stirrer to act as a reduction agent. The mixture was agitated for two hours until a white precipitate formed, and NH_4OH was gradually added to the mixture from a burette. The precipitate-containing solution was washed three times with methanol, collected, centrifuged, and allowed to dry overnight in a dust-free environment. Following that, the dried samples were calcined in a furnace at 1300°C before being collected by grinding them in an agate mortar. This same procedure was repeated to create x% Bi^{3+} (where x = 1.0, 1.5, 2.0, and 2.5) YZO samples by dissolving the required amount of $Bi(NO_3)_3.5H_2O$ in distilled water along with additional reagents.

3. RESULTS AND DISCUSSION

3.1 XRD Results

The XRD patterns of single-phase YZO: Pure and Bi^{3+} doped samples calcinated at temperature 1300^0C are shown in Figure 1. The reason for high calcinations temperature may be ascribed due to the fact that, higher calcinations temperature can easily produce nanoparticles bonding, formation of high-sized aggregates which affect the luminescence performance of the samples (Geng, Shang, Zhang, Lian, & Lin, 2013; Samuel & Kamal, 2022). The pyrochlore structure, denoted as $A_2B_2O_7$ (where $A=Y^{3+}$ and $B=Zr^{4+}$), aligns with the $Fd\bar{3}m$ space group, numbered as #227 (with Z = 8). The ions A, B, O, and O' reside in the 16c, 16d, 48f, and 8b crystallographic sites, respectively, inside this structure. The oxygen vacancy is represented by an empty '8a' site. The exact location of this vacancy is at the tetrahedral interstitial site between nearby B-site cations (Zr^{4+}). As a result, the coordination number of the A cation (La^{3+}) is still 8, while the coordination number of the B cation decreases to 6 from 8. ZrO_6 octahedra at the vertex corners and La^{3+} in the hexagonal holes constitute the framework of YZO's Ordered Pyrochlore (OP) structure, which creates a network of vertex corners and hexagonal holes (Tang et al., 2016).

Consequently, the introduction of Bi^{3+} ions through doping is anticipated to substitute Y^{3+} ions in the YZO structure, resulting in a singular-phase structure inclusive of the dopant ions. Figure 1 showcases diffraction peaks that closely align with the reported cubical phase of YZO (JCPDS-01-077-2117). Notably, there's no detection of a secondary phase, signifying the comprehensive dissolution of the Bi^{3+} ions within the YZO host lattice (Chen et al., 2018; Sashmeetha, Chitrarasu, & Thangadurai, 2019).

Consequently, the introduction of Bi^{3+} ions through doping is anticipated to substitute Y^{3+} ions in the YZO structure, resulting in a singular-phase structure inclusive of the dopant ions. Figure 1 showcases diffraction peaks that closely align with the reported cubical phase of YZO (JCPDS-01-077-2117). Notably, there's no detection of a secondary phase, signifying the comprehensive dissolution of the Bi^{3+} ions within the YZO host lattice (Chen et al., 2018; Sashmeetha, Chitrarasu, & Thangadurai, 2019).

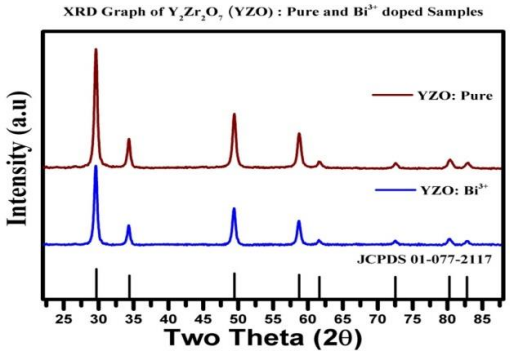

Figure 1. XRD graph of YZO: Pure and Bi^{3+} doped sample calcinated at 1300^0C.

Table 1 shows the average crystallite size which was estimated from the peak width (i.e, FWHM) of the few most intense peaks from the XRD pattern using Scherrer's equation (1).

$$\text{Average Crystallite Size, } D = \frac{0.9\lambda}{\beta \cos\theta} \text{ nm} \qquad (1)$$

Where λ is the wavelength of X-rays = 1.5406 A^0 and β is the corrected full width at half maximum (FWHM) of an observed peak and θ is the Bragg's Diffraction angle.

The average crystallite sizes are calculated using equation (1) and are found to be 20.63 nm for the pure YZO sample and 18.36 nm for the Bi^{3+} doped YZO sample. The distortion observed in the size is attributed to lattice strain, necessitating the introduction of charge-compensating defects and leading to the creation of oxygen vacancies. This arises from the mismatch in size between Y^{3+} ions of ionic radius 1.019 A^0 and Bi^{3+} ions of ionic radius 1.17 A^0. This phenomenon confirms the substitution of Bi^{3+} ions within the $Y_2Zr_2O_7$ (YZO) host lattice, replacing the Y^{3+} ions at tetrahedral sites without significantly altering the structure. (Kumar et al., 2018; Prasad, Walke, & Bhame, 2019; Shaik, Kumar, Chirauri, & Rao, 2022).

Table 1. Crystal Parameters of YZO: Pure and Bi^{3+} doped samples

Compound	a=b=c A^0	V $(A^0)^3$	Crystallite Size (nm)
YZO: Pure	5.21000	141.420	20.63
YZO: Bi^{3+}	5.21022	141.439	18.36

3.2 Morphology Results

The morphological studies of the YZO: Pure and Bi^{3+} doped phosphor powders were investigated by utilizing FEI Thermo Fisher Quanta 200F (SEM) instrument and are depicted in Figure 2. A collection of crystalline granules and particles are observed in the SEM images of the phosphorus.

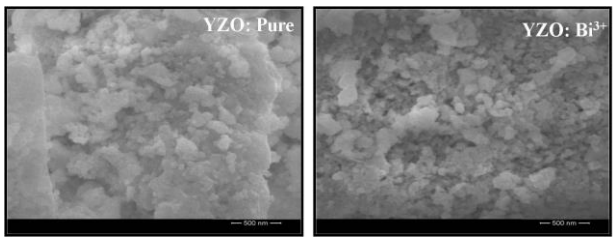

Figure 2. SEM images of (a) YZO: Pure, (b) YZO doped with Bi^{3+} sample

Owing to the phosphor particle aggregation that occurs during the calcinations, all the particles are discovered to be spherical in shape and the values of Avg. Particle size distribution of YZO pure and Bi^{3+} doped samples are 120 nm and 110.12 nm respectively. Figure 3 displays the particle size distribution between the Bi^{3+} doped and pure samples as determined by graphing histograms. The results revealed that the particle size decreases upon doping the sample with Bi^{3+}ions; this can be attributed to Coalescence effect. The difference in ionic radius between Y^{3+}& Bi^{3+} ions lead to this pseudo-distortion, resulting in a reduction in particle size (Edgar, 2007; Ju et al., 2011).

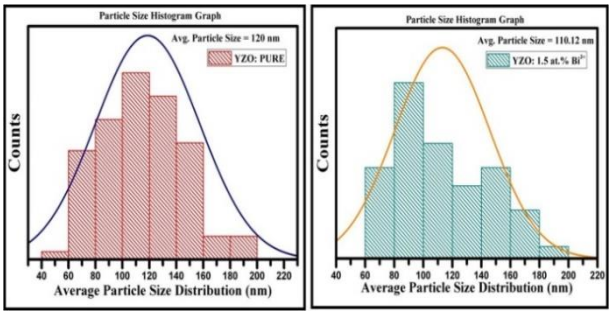

Figure 3. Avg. Particle Size distribution graphs of YZO: Pure and Bi^{3+} doped sample

3.3 Photoluminescence Results

The photoluminescence excitation and emission spectra of YZO: x at%. Bi^{3+} (x= 1.0, 1.5, 2.0 & 2.5) ions is depicted in Figure 4. Rare Earth ions such as bismuth are multipurpose since they can be used as activators and sensitizers. This indicates that it can both directly contribute to luminescence (activator role) and increase the luminescence of other ions (sensitizer role). The Bi^{3+} ions exhibit a variety of energy levels, including the ground state ($^1S_0$) and excited states ($^3P0$, $^3P_1$, $^3P_2$, and $^1P_1$). The luminous behaviour of Bi^{3+} is significantly influenced by the transitions between these states. Transitions between states are guided by spin-selection rules. For instance, the ΔS = 0 rule governs the transition from $^1S_0$ to $^1P_1$, while the $^1S_0$ to $^3P_0$ transition is prohibited because of the constant total angular momentum (ΔJ = 0) (Jafer et al., 2015; Ju et al., 2011). The $^1S_0$ to $^3P_1$ transition, which is frequently forbidden by spin-selection criteria, becomes permissible when singlet and triplet states are coupled. The experimental results are shown in Figure 4, which depicts the Photoluminescence spectra of YZO: x at% Bi^{3+} for different concentrations such as x= 1.0, 1.5, 2.0 & 2.5.

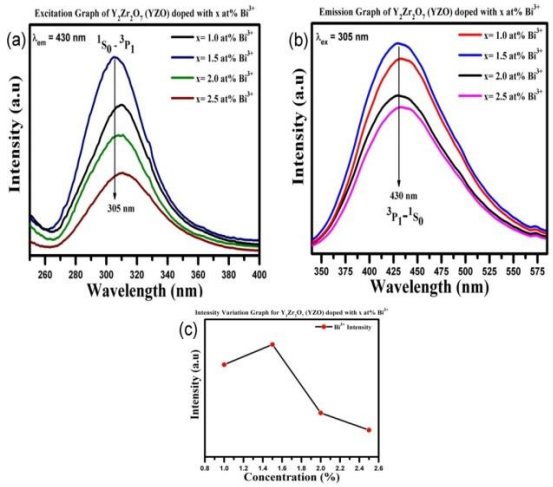

Figure 4. Photoluminescence Spectra (a) Excitation, (b) Emission and (c) Concentration Vs Emission Intensity graph of Bi^{3+} doped LZO samples

The $^1S_0$ to $^3P_1$ transition of Bi^{3+} ions is responsible for a broad excitation band that peaks at about 305 nm and extends from 250 nm to 400 nm. The excitation wavelength at which the emission spectra were recorded (λ_{ex} = 305 nm) revealed a unique emission band at around 430 nm (blue), which is associated with the $^3P_1 \rightarrow {}^1S_0$ transition of Bi^{3+} ions in the host structure. The intensity of emission at 430 nm increases as the concentration of Bi^{3+} ions rises to 1.5 at.%. Nevertheless, a concentration quenching effect causes the emission intensity to drop beyond this concentration. (Basina et al., 2023). Thus, the optimal composition is determined to be YZO: 1.5 at. % Bi^{3+} ions. Further, the relative emission intensities as a function of the dopant concentration is represented in Figure 4(c). However, the emission spectrum was used to determine the chromaticity colour coordinates in accordance with the CIE (Commission Internationale de l'Eclairage) 1932 in order to understand the luminous properties of the manufactured phosphor granules. Figure 5 shows the CIE diagram specifically for YZO doped with 1.5 at.% Bi^{3+}.

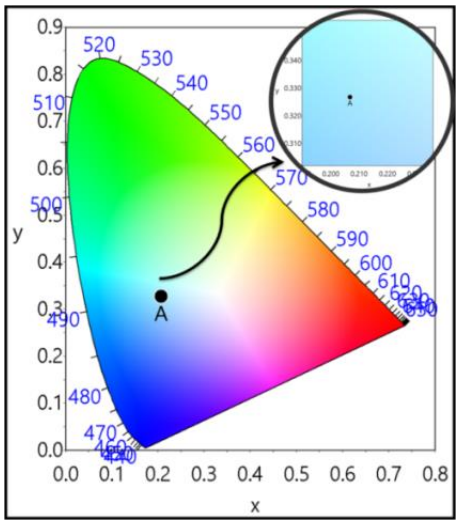

Figure 5. CIE Chromaticity diagram of optimized Bi^{3+} doped YZO sample

Using the (x, y) colour coordinates and specialized software, the CIE parameters were used to measure colour saturation. The color-correlated temperature (CCT) values (Figure 5) were calculated from the emission profiles of the prepared samples using a ratio that was derived from the chromaticity epicentre and the inverse slope line. (F. Du, Tang, Zhao, Du, & Xia, 2023; Suresh et al., 2018). The colour variables for optimized Bi^{3+} content (i.e., 1.5 at%) fall on the "Cyan" region with CIE coordinate values at X = 0.2068, Y = 0.3268, CCT value 14754 K, colour purity value 43.2%, and CRI value 37%, respectively (Li et al., 2022). Because of this, the YZO host sample doped with Bi^{3+} ions are thought to be appropriate for use in NUV blue emitting chips for display applications. Since the sample emits blue emission, it might be applicable for latent fingerprint detection, LED lighting and fluorescent lamps.

4. CONCLUSIONS

Yttrium Zirconate (YZO) phosphors powders doped with various concentrations of Bi^{3+} ions (x=1.0, 1.5, 2.0 & 2.5) were effectively synthesized through a straightforward "co-precipitation" method and subsequently annealed at 1300°C. XRD analyses demonstrated distinct crystallite size variations, with average sizes measuring 20.63 nm for pure YZO and 18.36 nm for the Bi^{3+} doped samples. SEM examinations highlighted spherical agglomeration morphology, ranging in size from 110 nm to 120 nm. The Photoluminescence studies unveiled the emission peak associated with the $^3P_1 \rightarrow {}^1S_0$ transition of Bi^{3+} ions, occurring at approximately 430 nm when excited at around 305 nm. Notably, there's a decline in emission intensity beyond a 1.5 at. % Bi^{3+} doping concentration due to a concentration quenching effect, leading to the identification of the optimal concentration as YZO: 1.5 at % Bi^{3+}. Evaluation of CIE color parameters indicated that the optimized Bi^{3+} content (1.5 at. %) exhibited characteristics within the "Cyan" region, with CIE coordinates at X = 0.2068, Y = 0.3268, along with color purity and CRI values of 43.2% and 37% respectively. Conclusively, the photoluminescence studies revealed that the prepared YZO sample doped with Bi^{3+} ions could be a promising material for the use in NUV blue emitting chips for display, LED and fluorescent lamp applications.

References:

Awater, R. H. P., & Dorenbos, P. (2017). The Bi^{3+} 6s and 6p electron binding energies in relation to the chemical environment of inorganic compounds. *Journal of Luminescence, 184*, 221-231. doi:10.1016/j.jlumin.2016.12.021

Basina, V. N. K., Yerramalla, N. R., Shaik, E. B., K, V., K, R. R., & Cole, S. (2023). Enhanced Luminescence and Energy Transfer of Bi^{3+}/Dy^{3+} Co-doped $La_2Zr_2O_7$ Nanophosphors for pc-LED Applications. *Physical Chemistry Research, 11*(1), 23-31. doi:10.22036/pcr.2022.333784.2050

Chen, Y., Xu, J., Xie, S., Tan, Z., Nie, R., Guan, Z., . . . Zhu, J. (2018). Ion Doping Effects on the Lattice Distortion and Interlayer Mismatch of Aurivillius-Type Bismuth Titanate Compounds. *Materials, 11*(5). doi:10.3390/ma11050821

Du, F., Tang, Z., Zhao, Q., Du, L., & Xia, W. (2023). $Ba_5GeO_4Br_6:Bi^{3+}$, a promising cyan phosphor for high-quality full-spectrum white light illumination. *Journal of Luminescence, 255*, 119592. doi:https://doi.org/10.1016/j.jlumin.2022.119592

Du, Q., Zhou, G., Zhou, H., & Yang, Z. (2012). Novel multiband luminescence of $Y_2Zr_2O_7:Eu^{3+}$, R^{3+} (R=Ce, Bi) orange–red phosphors via a sol–gel combustion approach. *Optical Materials, 35*(2), 257-262. doi:https://doi.org/10.1016/j.optmat.2012.08.014

Du, Q., Zhou, G., Zhou, J., Jia, X., & Zhou, H. (2013). Enhanced luminescence of novel $Y_2Zr_2O_7$:Dy^{3+} phosphors by Li+ co-doping. *Journal of Alloys and Compounds, 552*, 152-156. doi:https://doi.org/10.1016/j.jallcom.2012.10.074

Edgar, A. (2007). Luminescent Materials. In S. Kasap & P. Capper (Eds.), *Springer Handbook of Electronic and Photonic Materials* (pp. 983-996). Boston, MA: Springer US.

Gao, L., An, Y., Zhu, H., Wang, L., Chen, J., Wang, N., & Ou, G. (2011). Hydrothermal synthesis and photoluminescence properties of $Y_2Zr_2O_7$:Tb^{3+} phosphors. *Journal of Materials Science, 46*(5), 1337-1340. doi:10.1007/s10853-010-4924-3

Geng, D., Shang, M., Zhang, Y., Lian, H., & Lin, J. (2013). Color-Tunable and White Luminescence Properties via Energy Transfer in Single-Phase $KNaCa_2(PO_4)_2$:A (A = Ce^{3+}, Eu2+, Tb^{3+}, Mn2+, Sm^{3+}) Phosphors. *Inorganic Chemistry, 52*(23), 13708-13718. doi:10.1021/ic402305x

Jafer, R. M., Coetsee, E., Yousif, A., Kroon, R. E., Ntwaeaborwa, O. M., & Swart, H. C. (2015). X-ray photoelectron spectroscopy and luminescent properties of Y_2O_3:Bi^{3+} phosphor. *Applied Surface Science, 332*, 198-204. doi:https://doi.org/10.1016/j.apsusc.2015.01.009

Ju, G., Hu, Y., Chen, L., Wang, X., Mu, Z., Wu, H., & Kang, F. (2011). White-Light Generation and Energy Transfer in Y2O3:Bi,Eu Phosphor for Ultraviolet Light-Emitting Diodes. *Journal of The Electrochemical Society, 158*(10), J294. doi:10.1149/1.3615934

Kumar, B. V. N., Balla, P. K., Chirauri, S. K., Rao, T. K. V., Ramakrishna, Y., & Rao, K. R. (2018). Synthesis and characterization of copper particles decorated reduced graphene oxide nano composites for the application of supercapacitors. *AIP Conference Proceedings, 1992*(1). doi:10.1063/1.5047973

Li, Z.-J., Liu, B., Zhang, Y.-Y., Zhang, N.-N., Shi, Q., Wei, L., . . . Wang, X.-P. (2022). Cyan, deep red and white light emission generated by $SrLaGa_3O_7$:Bi^{3+}, $SrLaGa_3O_7$:Mn4+ and $SrLaGa_3O_7$:Bi^{3+}/Mn4+ phosphors. *Journal of Alloys and Compounds, 894*, 162455. doi:https://doi.org/10.1016/j.jallcom.2021.162455

Papan, J., Vuković, K., Ahrenkiel, S. P., Jovanović, D. J., & Dramićanin, M. D. (2017). Detailed study of structural and luminescent properties of $Y_{2-x}Eu_xZr_2O_7$ ($0 \leq x \leq 1$) nanophosphors. *Journal of Alloys and Compounds, 712*, 437-444. doi:10.1016/j.jallcom.2017.04.139

Prasad, R., Walke, P. S., & Bhame, S. D. (2019). Structural and optical studies on flowerlike strontium doped zinc oxide synthesized by hydrothermal method. *Materials Research Express, 6*(11), 1150b1158. doi:10.1088/2053-1591/ab4deb

Samuel, T., & Kamal, C. h. S. (2022). Investigation of Luminescence properties of Bi^{3+}, Dy^{3+} doped $LaAlO_3$ nanophosphors for radiation dosimetry applications. *International journal of health sciences, 6*(S1), 11638-11642. doi:10.53730/ijhs.v6nS1.7851

Sashmeetha, M., Chitrarasu, K., & Thangadurai, P. (2019). Tuning electrical properties of nanocrystalline $Y_2Zr_2O_7$ pyrochlores by engineering the size of their particles. *Ionics, 25*(12), 5949-5961. doi:10.1007/s11581-019-03138-7

Shaik, E. B., Kumar, B. V. N., Chirauri, S. K., & Rao, K. R. (2022). Realization of effective energy transfer and color tunability between Tb^{3+} and Eu^{3+} ions in $LaAlO_3$ host for LED display applications. *Journal of Materials Science: Materials in Electronics, 33*(1), 105-114. doi:10.1007/s10854-021-07257-8

Suresh, C., Nagabhushana, H., Darshan, G. P., Basavaraj, R. B., Kavyashree, D., Sharma, S. C., . . . Amith Yadav, H. J. (2018). Facile LaOF: Sm^{3+} based labeling agent and their applications in residue chemistry of latent fingerprint and cheiloscopy under UV–visible light. *Arabian Journal of Chemistry, 11*(4), 460-482. doi: 10.1016/j.arabjc.2017.09.014

Talari, S., Chirauri, S. K., Rambabu, A., & Ramachandra Rao, K. (2023). Development of single phase pink light-emitting Bi^{3+}/ Eu^{3+} co-doped $LaAlO_3$ phosphors for LED applications. *Materials Research Innovations, 27*(2), 61-68. doi:10.1080/14328917.2022.2079898

Talari, S., Chirauri, S. K., Reddy, P. V. S. S. S. N., & Rao, K. R. (2022). Photoluminescence studies of Bi^{3+}/Dy^{3+} co-doped $LaGaO_3$ nanophosphors for display device applications. *Materials Today: Proceedings, 52*, 2224-2227. doi: 10.1016/j.matpr.2021.08.042

Tang, Z., Wang, D., Khan, W. U., Du, S., Wang, X., & Wang, Y. (2016). Novel zirconium silicate phosphor $K_2ZrSi_2O_7$:Eu2+ for white light-emitting diodes and field emission displays. *Journal of Materials Chemistry C, 4*(23), 5307-5313. doi:10.1039/C6TC01449F

Ting, C.-C., Chiu, Y.-S., Chang, C.-W., & Chuang, L.-C. (2011). Visible and infrared luminescence properties of Er^{3+}-doped $Y_2Ti_2O_7$ nanocrystals. *Journal of Solid State Chemistry, 184*(3), 563-571. doi:10.1016/j.jssc.2011.01.001

Tong, Y., Chen, X., Wang, Q., & Huo, H. (2015). Crystal growth dynamics and structural characterization of re-doped $Y_2Zr_2O_7$ nanocrystals. *Materials Letters, 157*, 106-108. doi:10.1016/j.matlet.2015.05.089

Whittle, K. R., Cranswick, L. M. D., Redfern, S. A. T., Swainson, I. P., & Lumpkin, G. R. (2009). Lanthanum pyrochlores and the effect of yttrium addition in the systems $La_{2-x}Y_xZr_2O_7$ and $La_{2-x}Y_xHf_2O_7$. *Journal of Solid State Chemistry, 182*(3), 442-450. doi:10.1016/j.jssc.2008.11.008

Xiao, Z., Zhang, Z., Li, J., Zhang, B., Wu, B., Wang, F., . . . You, W. (2021). Preparation and luminescent properties of $Y_2Zr_2O_7:Eu^{3+}$ phosphor for W-LED application. *Applied Physics A, 127*(11), 866. doi:10.1007/s00339-021-05024-4

Zhang, A., Lü, M., Qiu, Z., Zhou, Y., & Ma, Q. (2008). Multiband luminescence of Eu^{3+} based on $Y_2Zr_2O_7$ nanocrystals. *Materials Chemistry and Physics, 109*(1), 105-108. doi: 10.1016/j.matchemphys.2007.10.042

K. Suresh
Department of Humanities & Basic Sciences, G. Pulla Reddy Engineering College (Autonomous),
Kurnool-518 007, A.P
India
kurudisuresh@gmail.com
ORCID 0000-0002-9779-0955

A. Ganesh
Department of Humanities & Basic Sciences, G. Pulla Reddy Engineering College (Autonomous),
Kurnool-518 007, A.P
India
ambaliganesh85@gmail.com
ORCID 0000-0002-2936-9245

B. V. Naveen Kumar
Shri Vishnu Engineering College for Women (Autonomous),
Bhimavaram – 534 202, A.P
India
bvnkbs@svecw.edu.in
ORCID 0000-0003-4700-5442

C. V. Krishna Reddy
Department of Physics,
Rayalaseema University,
Kurnool – 518 002, A.P, India
reddycvk02@yahoo.co.in
ORCID 0000-0001-7091-5482